

# MapGCLR: Geospatial Contrastive Learning of Representations for Online Vectorized HD Map Construction

Jonas Merkert<sup>1\*</sup>, Alexander Blumberg<sup>1\*</sup>, Jan-Hendrik Pauls<sup>1</sup>, and Christoph Stiller<sup>1</sup>

**Abstract**—Autonomous vehicles rely on map information to understand the world around them. However, the creation and maintenance of offline high-definition (HD) maps remains costly. A more scalable alternative lies in online HD map construction, which only requires map annotations at training time. To further reduce the need for annotating vast training labels, self-supervised training provides an alternative.

This work focuses on improving the latent birds-eye-view (BEV) feature grid representation within a vectorized online HD map construction model by enforcing geospatial consistency between overlapping BEV feature grids as part of a contrastive loss function. To ensure geospatial overlap for contrastive pairs, we introduce an approach to analyze the overlap between traversals within a given dataset and generate subsidiary dataset splits following adjustable multi-traversal requirements. We train the same model supervised using a reduced set of single-traversal labeled data and self-supervised on a broader unlabeled set of data following our multi-traversal requirements, effectively implementing a semi-supervised approach. Our approach outperforms the supervised baseline across the board, both quantitatively in terms of the downstream tasks vectorized map perception performance and qualitatively in terms of segmentation in the principal component analysis (PCA) visualization of the BEV feature space.

**Index Terms**—Online HD Map Construction, Automated Driving, Semi-Supervised Learning, Contrastive Learning

## I. INTRODUCTION

High-definition (HD) maps remain highly relevant as foundation for the planning task in current software stacks for autonomous vehicles [1]. Compared to standard-definition (SD) maps, HD maps provide more detailed, precise, and semantic information, including, but not limited to, the actual geometry of road elements, such as lane dividers or road boundaries, as well as their relations [2].

The creation and constant maintenance of such HD maps remain resource-intensive, requiring regular mapping using mobile mapping platforms equipped with highly precise sensors and reference global localization systems, as well as at least partial manual annotations.

Hence, recent research has focus on constructing HD maps while driving. These online methods predict vectorized HD map-like representations of the local surrounding in real-time based on 360° vision input [3, 4, 5], as well as possible prior knowledge [6, 7]. Although this dramatically reduces the necessity for valid HD maps on a global scale, these learned

\*These authors contributed equally to this work.

<sup>1</sup>Institute of Measurement and Control Systems, Karlsruhe Institute of Technology (KIT), Karlsruhe, Germany  
{alexander.blumberg, jonas.merkert, jan-hendrik.pauls, christoph.stiller}@kit.edu

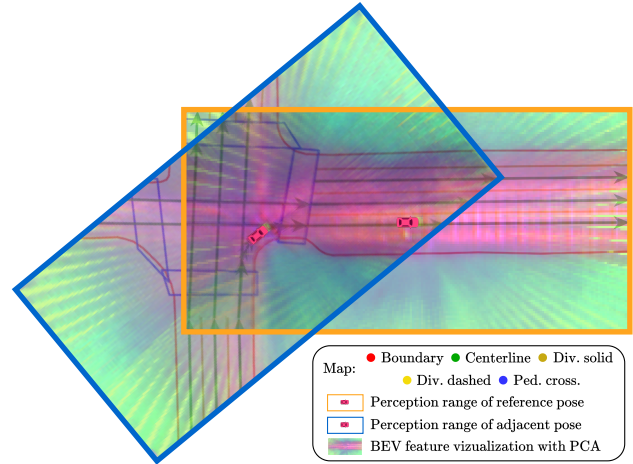


Fig. 1: Overlapping BEV feature grids visualized using PCA. In the background, we depict ground truth map labels with road boundaries, lane dividers, centerlines and pedestrian crossing. Both the geospatial consistency between overlapping BEV feature spaces as well as their alignment with the target road layout can be recognized.

approaches still rely on a well-distributed set of training data and are susceptible to missing corner cases. Perspectively, providing such training data remains the major bottleneck for scalable online HD map construction.

This work strikes to overcome this bottleneck by focusing on improving the intermediate birds-eye-view (BEV) feature grid representation present in vectorized HD map construction models. Using self-supervised contrastive learning, we enforce a consistent latent space between geospatially overlapping BEV feature grids.

The main contributions of this work are:

- As necessary foundation for geospatial consistency, we propose an approach to analyze the geospatial overlap between traversals within a given dataset. This facilitates the definition of novel dataset splits by geospatial overlap requirements across traversals.
- We introduce a novel semi-supervised training regime for BEV feature grid encoders, leveraging geospatial relations between different poses and their respective feature grids using a contrastive loss function.
- We evaluate our approach on the Argoverse 2 dataset against a set of supervised baselines, showing quantitative gains between 13% and 42%. Qualitatively, we demonstrate alignment of the latent space both across traversals and with target HD maps.

## II. RELATED WORK

In the following section, we cover relevant prior work on semi-supervised learning and online HD map construction.

### A. Semi-supervised Learning

In the semi-supervised learning paradigm, a large unlabeled dataset and a small labeled dataset are combined to train a model, whereas in self-supervised learning (SSL), pseudo-labeling is often used to generate labels from the data itself, and therefore, no real labels are needed. In general, two approaches are examined in semi-supervised learning: multi-stage training and one-stage training. In the multi-stage setup, the model is first trained unsupervised or self-supervised to learn generic features and then finetuned supervised for the actual downstream task [8, 9]. In contrast, in one-staged training, labeled and unlabeled data are mixed within a batch and processed with different data flows, resulting in different loss terms for the labeled and unlabeled data [10, 11, 12].

While semi-supervised learning have had a strong influence on image classification and object detection in previous years, recent research has extended these concepts to the domain of autonomous driving. Several SSL techniques, such as teacher-student architectures [13], feature distillation [14] and contrastive learning [15] have been leveraged to improve the performance of semantic BEV segmentation or 3D object detection in the autonomous driving domain.

In the online HD map construction domain, only two approaches leverage semi-supervised learning. PseudoMapTrainer [16] utilizes sensor data to generate a coherent mesh grid of Gaussian surfels. By rendering these surfels into a BEV segmentation, pseudo-labels are generated and used to pre-train the model in a semi-supervised manner. In contrast, Lilja et al. [17] employ a semi-supervised framework built on a teacher-student architecture. To improve the soft labels of the teacher network, a temporal pseudo-label fusion is introduced, which aggregates these labels over time. Both methods leverage pseudo-labels generated from sensor data in a semi-supervised setup to boost model performance. In contrast, our approach exploits geospatial consistency to learn meaningful BEV features by training the encoder with an additional self-supervised objective, thereby improving performance on the online HD map construction task. Another key distinction is that we utilize a vector-based method that directly predicts map elements as polylines, whereas PseudoMapTrainer [16] and Lilja et al. [17] employ a semantic segmentation-based approach.

### B. Online HD Map Construction

HMapNet [18] first proposed a multi-stage pipeline to predict a set of vectorized map elements by transforming camera images into a BEV grid and utilizing semantic segmentation with a heuristic postprocessing. Subsequent studies, including VectorMapNet [19] and MapTR [3], utilize the transformer-style architecture DETR [20] as a decoder to directly predict map elements as polylines. Whereas VectorMapNet [19] utilizes an autoregressive approach to predict each instance, MapTR [3] introduces a hierarchical

query design to predict all polylines in a single step. Based on this hierarchical query design, MapTRv2 [4], MapQR [21] and DAMap [22] extend this approach with auxiliary tasks, advanced query design, or loss function adaptations.

While these single-shot approaches utilize only current sensor information, recent studies attempt to boost performance by leveraging information from previous predictions in the form of short-term memory. HMapNet [18] introduces short-term memory by fusing BEV features with max-pooling, whereas StreamMapNet [23] goes one step further by establishing a memory buffer with a gated recurrent unit (GRU) and storing BEV features and decoder queries from the previous predictions. By establishing a tracking mechanism for the predicted map elements and BEV features, MapTracker [5] significantly improves the map construction performance and achieves state-of-the-art performance.

To address the limitations of single-shot and short-term memory approaches, global map priors are used to enhance the quality of predictions, particularly in long-range scenarios. SMERF [24], SDTagNet [7] and M3TR [6] utilize SD or outdated HD maps to enhance recent sensor information. In contrast, HRMapNet [25] exploits multi-traversals by storing BEV features or rasterized polylines into a global map. RTMap [26] extends the leverage of multi-traversals for online HD map construction by adding uncertainties to local predictions. Our objective is to investigate SSL approaches that exploit geospatial consistency from multi-traversals to organize the BEV feature space in a meaningful way. To this end, we develop a semi-supervised framework based on a single-shot architecture that does not rely on previous predictions.

## III. METHODOLOGY

This section describes the creation of a multi-traversal dataset split and our geospatial contrastive learning strategy to utilize geospatial consistency in a semi-supervised learning pipeline.

### A. Geospatial Multi-traversal Split

As outlined in Section II, recent research on HD map construction has focused on leveraging temporal or spatial consistency to improve model predictions. However, employing spatial consistency necessitates storing previous predictions at specific locations, resulting in vastly increased memory consumption and model complexity.

**Single- and Multi-traversal Classification:** To directly utilize spatial consistency across traversals, we propose a method for examining the geospatial overlap between traversals within a dataset. This facilitates creating single- and multi-traversal splits based on these overlaps. Initially, we transform all poses into a global reference frame and divide the scenario logs into multiple large areas, e.g. according to the various cities. Based on these divisions, we classify each log into single- and multi-traversals using the perception range of the vehicle. Consequently, we calculate a bounding box for each pose based on the vehicle heading denoting the

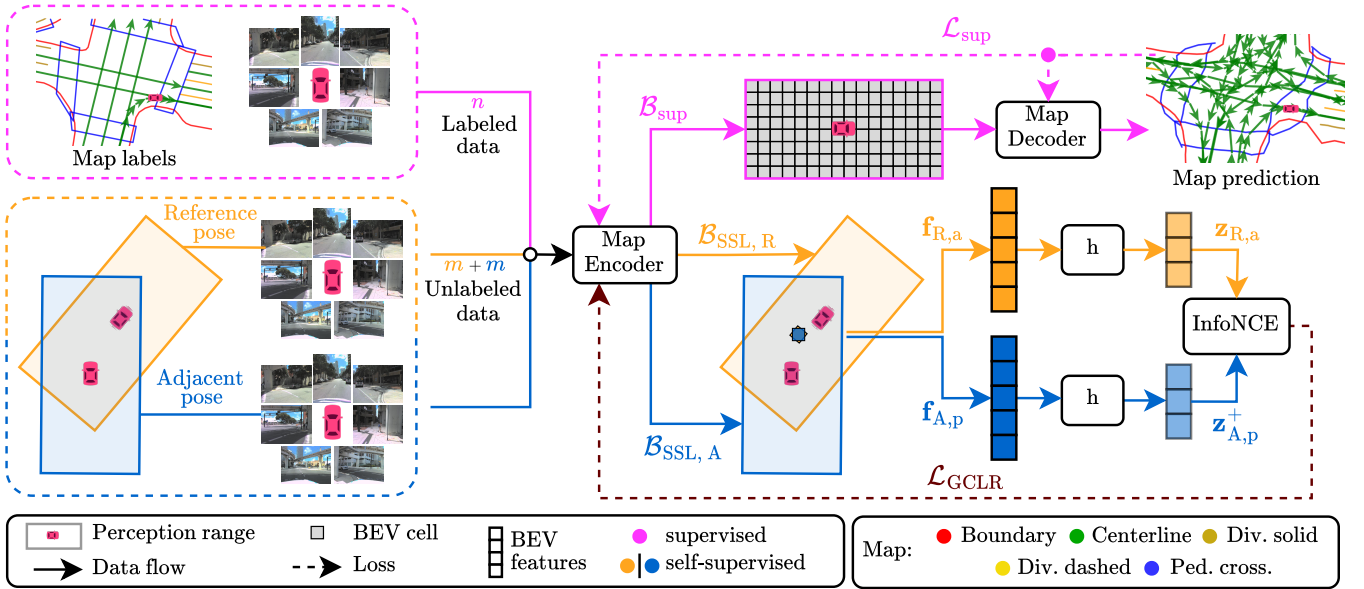


Fig. 2: Schematic overview of the semi-supervised learning pipeline. Data flows are shown for supervised (pink) and self-supervised (blue, orange) samples.  $B$  denotes BEV grids with cell features  $f$  and embeddings  $z$  produced by projection head  $h$ . Losses  $\mathcal{L}_{sup}$  and  $\mathcal{L}_{GCLR}$  correspond to supervised and self-supervised branches, respectively.

driving direction, with  $\pm x$  meters in the lateral and  $\pm y$  meters in the longitudinal directions with respect to the vehicle’s pose, and merge all the bounding boxes of each traversal into a single polygon. A traversal is classified as a multi-traversal if the corresponding polygon intersects at least one polygon from another traversal. If no other traversals intersects, the traversal is classified as a single-traversal. One exception is made: if only two drives intersect each other, both are classified as single-traversals. This exception is made since such that traversals provide only limited additional variety to effectively train for geospatial consistency and to enable an adequate size of the single-traversal split.

**Spatial Graph Creation:** To efficiently manage these overlaps, we construct a spatial graph  $G = (V, E)$ . Each vertex  $v \in V$  represents a vehicle pose, and an edge  $e_{ij} \in E$  is drawn between two poses if they satisfy the spatial intersection criterion. Specifically, we calculate the Intersection over Union (IoU) between the perception grids of  $P_i$  and  $P_j$ . Edges are maintained only for pairs in which the overlap falls within a predefined range  $[\text{IoU}_{\min}, \text{IoU}_{\max}]$ . Constraining the minimum and maximum values of the IoU ensures that the overlapping areas are sufficiently related but not identical.

### B. Geospatial Contrastive Learning

To leverage geospatial consistency in a multi-traversal setup, we propose a SSL approach based on the contrastive learning framework SimCLR [8]. Unlike traditional contrastive learning methods that rely on image augmentations, our approach exploits the inherent spatial correspondences that emerge when the same geospatial area is traversed multiple times. Specifically, we treat overlapping poses as natural augmentations and call them *reference-adjacent* pairs, where the *reference* denotes the reference pose and *adjacent* denotes

another pose with intersecting perception range being an adjacent in the spatial graph.

**Positive and Negative Sample Definition:** Contrastive learning aims to organize the feature space by pulling similar data points together while pushing dissimilar points apart. This is achieved through positive and negative pair definitions relative to an anchor [8]. In our approach, the BEV grids  $B_{SSL,R}$  and  $B_{SSL,A}$  are predicted for the reference and adjacent poses based on the corresponding camera data. To employ geospatial consistency, we transform these BEV grids with respect to the vehicle’s position and heading into a global coordinate system and utilize the BEV cells from these transformed grids to define positive and negative pairs relative to an anchor BEV cell. A BEV cell  $c_p$  with feature vector  $f_p$  is considered a positive sample with respect to an anchor BEV cell  $c_a$  with feature vector  $f_a$  if both cells represent the same geospatial location and therefore should exhibit similar features. Conversely, a BEV cell  $c_n$  with feature vector  $f_n$  is considered a negative sample if the cells do not share spatial correspondence, resulting in dissimilar features.

**Sampling Strategy:** Starting from two intersecting poses, the reference pose  $R$  and the adjacent pose  $A$ , we categorize each of the BEV cells  $c$  in the BEV grids  $B_{SSL,R}$  and  $B_{SSL,A}$  as inliers or outliers with respect to the overlap area. For positive pairs, we randomly sample BEV cells  $c$  from our *reference* BEV grid  $B_{SSL,R}$  that lie within the overlap area and serve as anchor points. For each of these anchor points, we perform a nearest-neighbor search in the *adjacent* BEV grid to identify the corresponding positive cell at the same geospatial location. In contrast, the negative pairs are randomly sampled from both the reference and adjacent grid, explicitly excluding the anchor and positive cells to ensure

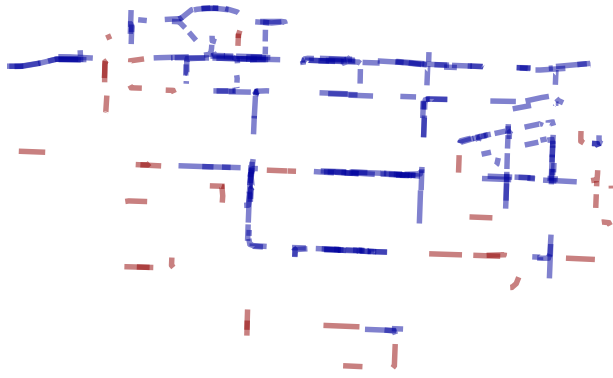
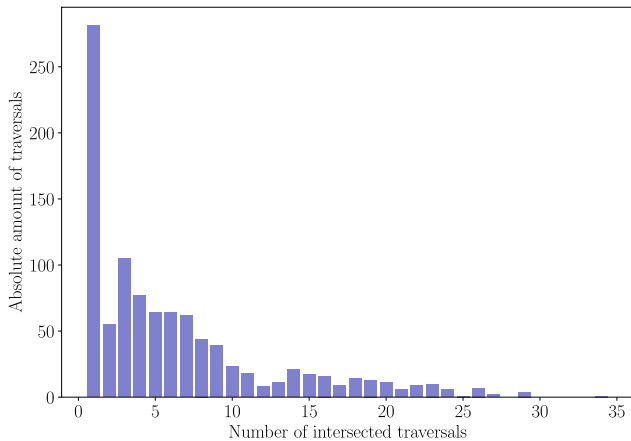


Fig. 3: Single- and multi-traversals within Argoverse 2: The histogram on the left shows the general distribution of intersecting drive logs. On the right, we visualize the geospatial distribution of single- (red) and multi-traversals (blue) within Miami.

the representation of distinct geospatial locations.

**Loss Function:** Based on the sampling of positive and negative cell pairs, we employ the InfoNCE loss [27] to train the network. Analogous to SimCLR [8], we utilize a projection head  $h$  and transform each BEV cell feature  $\mathbf{f}$  into another feature space  $\mathbf{z} \in \mathcal{Z}$  and therefore decouple the learning domain from the application domain. Given an anchor cell embedding  $\mathbf{z}_i$  and its corresponding positive cell embedding  $\mathbf{z}_i^+$ , along with a set of negative embeddings  $\{\mathbf{z}_k^-\}_{k=1}^K$ , the geospatial contrastive loss  $\mathcal{L}_{\text{GCLR}}$  is formulated as

$$\mathcal{L}_{\text{GCLR}} = -\log \frac{\exp\left(\frac{\text{sim}(\mathbf{z}_i, \mathbf{z}_i^+)}{\tau}\right)}{\exp\left(\frac{\text{sim}(\mathbf{z}_i, \mathbf{z}_i^+)}{\tau}\right) + \sum_{k=1}^K \exp\left(\frac{\text{sim}(\mathbf{z}_i, \mathbf{z}_k^-)}{\tau}\right)}, \quad (1)$$

where  $\text{sim}(\cdot, \cdot)$  denotes the cosine similarity and  $\tau$  is a temperature parameter. This objective encourages the network to produce similar embeddings for BEV cells corresponding to the same geospatial location across different traversals while pushing apart the embeddings of cells from different locations. An overview of the geospatial contrastive learning approach for a positive cell pair is shown with orange and blue colors for the *reference* and *adjacent*, respectively, in Fig. 2.

### C. Semi-supervised Training Regime

This work aims to exploit SSL to boost the performance of the online HD map construction task. We propose to combine supervised and self-supervised methods in online HD map construction under the assumption that we have access to two distinct datasets: a small, labeled dataset containing camera images with corresponding ground truth HD map labels, which is expensive to annotate, as well as an easily scalable unlabeled dataset containing only camera images and vehicle poses. Fig. 2 shows an overview of the proposed semi-supervised learning pipeline, where three distinct data flows are visualized: the supervised data flow (pink) and two

self-supervised data flows for anchor and positive samples (orange and blue).

**Architecture and Batch Composition:** From an architectural perspective, we adopt the single-shot HD map construction model MapTRv2 [4], which follows an encoder-decoder structure. For each training batch, we sample  $n$  poses with their corresponding camera images and ground truth map labels from the labeled dataset and fill-up the batch with samples from the unlabeled dataset. Since our contrastive approach requires *reference-adjacent* pose pairs, where each reference pose  $R$  is matched with a geospatially intersecting pose  $A$ , the number of unlabeled samples is constrained to be divisible by two. Consequently, each batch contains a total of  $n + 2m$  samples, where  $n$  denotes the number of supervised samples and  $2m$  denotes the number of self-supervised samples organized as  $m$  *reference-adjacent* pairs.

**Feature Extraction and Lifting:** All samples are passed through a MapTRv2 [4] map encoder, which consists of a ResNet-50 [28] backbone for extracting image features and a lifting module for transforming these features into BEV representation. As a result, we obtain BEV grids for each sample: Specifically,  $n$  BEV grids  $\mathcal{B}_{\text{sup}}$  for the supervised samples,  $m$  BEV grids  $\mathcal{B}_{\text{SSL,R}}$  for the reference poses, and  $m$  BEV grids  $\mathcal{B}_{\text{SSL,A}}$  for the adjacent poses from the unlabeled dataset.

**Supervised Learning Branch:** From this point, the data flow diverges between labeled and unlabeled data. The labeled data, represented by BEV grids  $\mathcal{B}_{\text{sup}}$ , flows directly into a map decoder based on MapTRv2 [4]. This decoder utilizes a transformer-based architecture to predict map elements in the form of polylines with corresponding class labels. The supervised loss  $\mathcal{L}_{\text{sup}}$ , strictly following MapTRv2 [4], is computed based on the predicted polylines and classes and backpropagated through both the map decoder and map encoder modules. For each batch,  $\mathcal{L}_{\text{sup}}$  is calculated as the sum over all  $n$  labeled samples.

**Self-supervised Learning Branch:** For the unlabeled data, the generated BEV grids  $\mathcal{B}_{\text{SSL,R}}$  and  $\mathcal{B}_{\text{SSL,A}}$  from the refer-

TABLE I: Comparison of the supervised and semi-supervised training strategies for the categories divider dashed (dsh), solid (sol), boundary (bou), centerline (cen) and pedestrian crossing (ped). The first two columns denote the share of supervised training data as well as the use of self-supervised learning (SSL).

Sup. Data	SSL	AP <sub>dsh</sub>	AP <sub>sol</sub>	AP <sub>bou</sub>	AP <sub>cen</sub>	AP <sub>ped</sub>	mAP	$\Delta_{\text{abs}}$	$\Delta_{\text{rel}}$
2.5%	✗	4.3	5.0	9.6	11.9	1.5	6.5		
	✓	5.2	6.7	12.2	17.0	1.6	8.5	+2.0	+31%
5%	✗	10.3	9.5	20.5	19.1	7.3	13.3		
	✓	15.4	18.7	24.8	25.4	9.9	18.9	+5.6	+42%
10%	✗	17.6	20.9	31.9	27.1	12.4	22.0		
	✓	20.8	30.5	34.5	32.4	18.2	27.3	+5.3	+24%
20%	✗	27.2	32.1	38.9	34.7	22.3	31.0		
	✓	31.2	38.8	39.9	37.5	26.9	34.9	+3.9	+13%
30%	✗	34.3	39.8	41.7	38.7	28.7	36.6		
40%	✗	37.8	43.7	43.9	41.2	32.7	39.8		

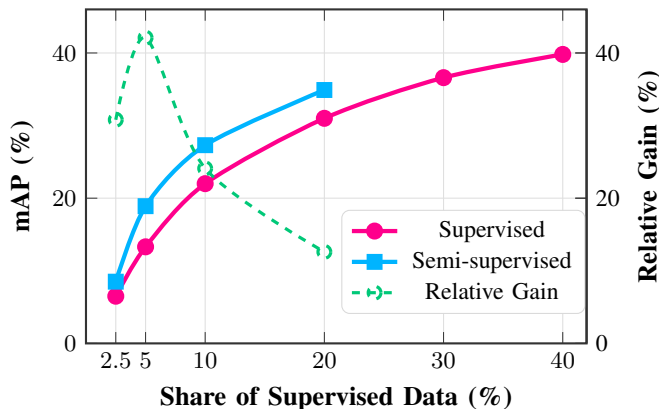


Fig. 4: Performance scaling and relative gains across increasing share of supervised data.

ence and adjacent pose are used to sample the positive and negative cell pairs and compute the geospatial contrastive loss  $\mathcal{L}_{\text{GCLR}}$ , as described in Section III-B. Again,  $\mathcal{L}_{\text{GCLR}}$  is computed as sum over all  $m$  unlabeled pose pairs.

**Combined Loss Function:** The overall semi-supervised loss  $\mathcal{L}_{\text{semi}}$  for each batch is determined by the weighted combination of the supervised loss  $\mathcal{L}_{\text{sup}}$  and geospatial contrastive loss  $\mathcal{L}_{\text{GCLR}}$ , with weighting factors  $\lambda_{\text{sup}}$  and  $\lambda_{\text{GCLR}}$ , respectively:

$$\mathcal{L}_{\text{semi}} = \lambda_{\text{sup}}\mathcal{L}_{\text{sup}} + \lambda_{\text{GCLR}}\mathcal{L}_{\text{GCLR}}. \quad (2)$$

These weighting factors serve two purposes: they scale both loss terms into comparable ranges and allow us to control the relative influence of supervised and SSL on the overall training objective. This formulation enables the model to benefit from both the precise supervisory signal from labeled data and the geospatial consistency constraints learned from unlabeled multi-traversal data.

#### IV. EVALUATION

##### A. Experimental Setup

We evaluate our approach on Argoverse 2 [29], a well-established dataset for supervised online HD map construction [4, 5]. However, its fit for semi-supervised training as described in Section III-C remains to be investigated.

**Multi-Traversal Analysis:** In order for Argoverse 2 to qualify as a solid foundation for our semi-supervised experiments, we require a great number of multi-traversals present within the dataset. We employ our classification approach as described in Section III-A, providing us with deep insight into the composition of the dataset as visualized both quantitatively and qualitatively in Fig. 3. The qualitative visualization demonstrates the effectiveness of our classification step with majorly overlapping sections consistently being classified as multi-traversal. The histogram of Fig. 3 states the presence of a vast portion of traversals within the dataset to include multiple intersections with other traversals, making Argoverse 2 well suited for evaluating our training approaches.

**Dataset Splits:** Based on our single- and multi-traversal classification from in Section III-A, we utilize all logs classified as multi-traversal as our self-supervised split, ignoring labels present for this portion in all experiments all together. Among those classified as single-traversal, we initially select logs at random to form a static validation set comprising 10 % of the total number of poses in the dataset, always including entire logs. From the remaining single-traversals, we randomly shuffle and sequentially assign complete logs to our supervised subsets, creating splits that comprise 2.5 %, 5 %, 10 %, and 20 % of the total number of poses in the dataset. We define these static sets this way to ensure lower percentage supervised subsets to also always be a subset of all its higher percentage subsets, reducing selection bias between subsets. Higher percentage supervised subsets (30 % and 40 % splits) are defined to provide a trend of the supervised performance, include parts of the self-supervised split and are therefore not usable for self-supervised training.

##### B. Quantitative Results

To quantify the benefit of our semi-supervised training regime, we employ MapTRv2 [4] trained with its original purely supervised training regime as baseline. To level the playing field, we provide both models with equal access to labeled training data, varying the percentage based on the split at hand. Table I presents the increase in performance by utilizing self-supervised training (SSL) compared to the baseline. The benefit of the proposed method is also visualized in Fig. 4.

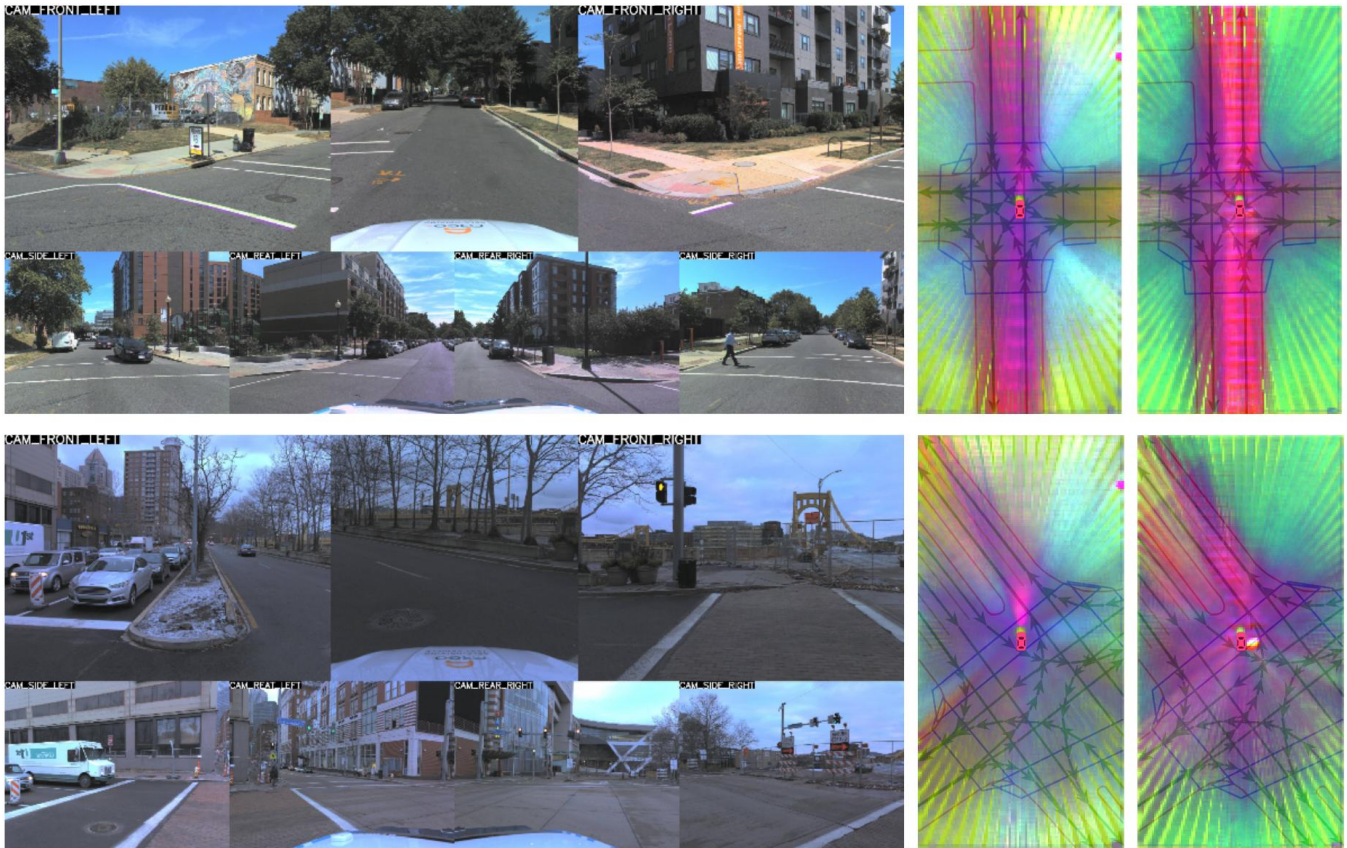


Fig. 5: Qualitative visualization of PCA of the supervised baseline (middle) and our semi-supervised approach (right) with ground-truth labels in the background for reference. Input surround view on the left, 20 % supervised split.

Using the proposed self-supervised contrastive learning with additional unlabeled training data significantly improves the online HD map construction performance across all conducted experiments, yielding relative gains between 13 % and 42 %. As apparent in Fig. 4, the benefit is particularly distinct for small amounts of labeled data, where it is almost as good as doubling the amount of labeled training data.

### C. Qualitative Results

We visualize the BEV feature grid using principal component analysis (PCA) to qualitatively assess its spatial and semantic structure, as coherent and well-separated feature organization is indicative of effective representation learning and typically correlates with improved downstream performance [30]. The PCA is calculated across all scenes of the validation set to provide consistent results.

Two example scenes can be observed in Fig. 5. While the feature separation of both the baseline and our semi-supervised approach appears cleaner in the less complex upper scene, ours delivers stronger contrasts in both scenes, especially around road borders. Additionally, a stronger separation of the ego lane can be observed.

Interestingly, we also observe an unexpected feature cluster in the baseline output in the top right of its grid, that always appear at identical grid coordinates, a curiosity that is effectively eliminated with our approach, since it contradicts geospatial consistency.

## V. CONCLUSION

We presented an effective approach to boost online vectorized HD map construction performance using geospatial contrastive learning with unlabeled data. It leverages the geospatial consistency across traversals in BEV feature space.

By implementing an effective single- and multi-traversal classification for autonomous driving datasets, we not only pave ground work for our own semi-supervised training regime, but also provided statistical insights into the Argoverse 2 dataset in particular.

Our semi-supervised training regime outperforms the supervised baseline across the board, demonstrating the effectiveness of our approach both quantitatively in terms of mAP and qualitatively with improved separation in BEV feature space.

A major prerequisite for our approach is the availability of highly accurate (relative) localization, which is also a crucial requirement for purely supervised models that use a ground truth map [31]. While this feature is unfortunately missing in some of the largest autonomous driving datasets that would allow scaling our idea even further [32], our contrastive loss formulation could also be used to refine relative poses, mitigating this bottleneck at least partially. Further work can also extend our approach by incorporating SSL methods into the transformer-decoder of the model. This could propagate

the benefits beyond the intermediate BEV representation, boosting the final map prediction performance of the model.

#### REFERENCES

- [1] S. Kato, S. Tokunaga, Y. Maruyama, S. Maeda, M. Hirabayashi, Y. Kitsukawa, et al., “Autoware on board: Enabling autonomous vehicles with embedded systems,” in *2018 ACM/IEEE 9th International Conference on Cyber-Physical Systems (ICCPs)*, 2018, pp. 287–296.
- [2] F. Poggenhans, J.-H. Pauls, J. Janosovits, S. Orf, M. Naumann, F. Kuhnt, et al., “Lanelet2: A high-definition map framework for the future of automated driving,” in *2018 21st International Conference on Intelligent Transportation Systems (ITSC)*, Maui, HI, USA: IEEE Press, 2018, pp. 1672–1679, ISBN: 978-1-7281-0321-1.
- [3] B. Liao, S. Chen, X. Wang, T. Cheng, Q. Zhang, W. Liu, et al., “Maptr: Structured modeling and learning for online vectorized hd map construction,” in *International Conference on Learning Representations*, 2023.
- [4] B. Liao, S. Chen, Y. Zhang, B. Jiang, Q. Zhang, W. Liu, et al., “Maptrv2: An end-to-end framework for online vectorized hd map construction,” *International Journal of Computer Vision*, pp. 1–23, 2024.
- [5] J. Chen, Y. Wu, J. Tan, H. Ma, and Y. Furukawa, “MapTracker: Tracking with Strided Memory Fusion for Consistent Vector HD Mapping,” in *Computer Vision – ECCV 2024*, A. Leonardis, E. Ricci, S. Roth, O. Russakovsky, T. Sattler, and G. Varol, Eds., Cham: Springer Nature Switzerland, 2025, pp. 90–107, ISBN: 978-3-031-72658-3.
- [6] F. Immel, R. Fehler, F. Bieder, J.-H. Pauls, and C. Stiller, “M3tr: A generalist model for real-world hd map completion,” *IEEE Robotics and Automation Letters*, vol. 10, no. 12, pp. 12 541–12 548, 2025.
- [7] F. Immel, J.-H. Pauls, R. Fehler, F. Bieder, J. Merkert, and C. Stiller, “Sdtagnet: Leveraging text-annotated navigation maps for online hd map construction,” 2025.
- [8] T. Chen, S. Kornblith, M. Norouzi, and G. Hinton, “A simple framework for contrastive learning of visual representations,” in *Proceedings of the 37th International Conference on Machine Learning*, ser. ICML’20, vol. 119, JMLR.org, Jul. 2020, pp. 1597–1607.
- [9] M. Caron, H. Touvron, I. Misra, H. Jégou, J. Mairal, P. Bojanowski, et al., “Emerging properties in self-supervised vision transformers,” in *Proceedings of the International Conference on Computer Vision (ICCV)*, 2021.
- [10] P. Tang, C. Ramaiah, Y. Wang, R. Xu, and C. Xiong, “Proposal learning for semi-supervised object detection,” in *Proceedings of the IEEE/CVF Winter Conference on Applications of Computer Vision (WACV)*, Jan. 2021, pp. 2291–2301.
- [11] M. Xu, Z. Zhang, H. Hu, J. Wang, L. Wang, F. Wei, et al., “End-to-end semi-supervised object detection with soft teacher,” in *Proceedings of the IEEE/CVF International Conference on Computer Vision (ICCV)*, Oct. 2021, pp. 3060–3069.
- [12] B. Chen, W. Chen, S. Yang, Y. Xuan, J. Song, D. Xie, et al., “Label matching semi-supervised object detection,” in *Proceedings of the IEEE/CVF Conference on Computer Vision and Pattern Recognition (CVPR)*, Jun. 2022, pp. 14 381–14 390.
- [13] J. Zhu, L. Liu, Y. Tang, F. Wen, W. Li, and Y. Liu, “Semi-supervised learning for visual bird’s eye view semantic segmentation,” in *2024 IEEE International Conference on Robotics and Automation (ICRA)*, 2024, pp. 9079–9085.
- [14] S. Sirko-Galouchenko, A. Boulch, S. Gidaris, A. Bursuc, A. Vobecky, P. Pérez, et al., “Occfeat: Self-supervised occupancy feature prediction for pretraining bev segmentation networks,” in *Proceedings of the IEEE/CVF Conference on Computer Vision and Pattern Recognition (CVPR) Workshops*, Jun. 2024, pp. 4493–4503.
- [15] Z. Leng, J. Yang, Z. Ren, and B. Zhou, “Bevcon: Advancing bird’s eye view perception with contrastive learning,” *IEEE Robotics and Automation Letters*, vol. 10, no. 4, pp. 3158–3165, 2025.
- [16] C. Löwens, T. Funke, J. Xie, and A. P. Condurache, “Pseudomap-trainer: Learning online mapping without hd maps,” in *Proceedings of the IEEE/CVF International Conference on Computer Vision (ICCV)*, Oct. 2025, pp. 5263–5272.
- [17] A. Lilja, E. Wallin, J. Fu, and L. Hammarstrand, “Exploring semi-supervised learning for online mapping,” *2025 IEEE/CVF Conference on Computer Vision and Pattern Recognition Workshops (CVPRW)*, pp. 2468–2478, 2024.
- [18] Q. Li, Y. Wang, Y. Wang, and H. Zhao, “Hdmapnet: An online hd map construction and evaluation framework,” in *2022 International Conference on Robotics and Automation (ICRA)*, Philadelphia, PA, USA: IEEE Press, 2022, pp. 4628–4634.
- [19] Y. Liu, T. Yuan, Y. Wang, Y. Wang, and H. Zhao, “Vectormapnet: End-to-end vectorized hd map learning,” in *International conference on machine learning*, PMLR, 2023.
- [20] N. Carion, F. Massa, G. Synnaeve, N. Usunier, A. Kirillov, and S. Zagoruyko, “End-to-end object detection with transformers,” in *Computer Vision – ECCV 2020: 16th European Conference, Glasgow, UK, August 23–28, 2020, Proceedings, Part I*, Glasgow, United Kingdom: Springer-Verlag, 2020, pp. 213–229, ISBN: 978-3-030-58451-1.
- [21] Z. Liu, X. Zhang, G. Liu, J. Zhao, and N. Xu, “Leveraging enhanced queries of point sets for vectorized map construction,” in *European Conference on Computer Vision*, 2024.
- [22] J. Dong, C. Li, Y. Lin, J. Fu, S. Zhou, and N. Zheng, “Damp: Distance-aware mapnet for high quality hd map construction,” in *Proceedings of the IEEE/CVF International Conference on Computer Vision*, 2025.
- [23] T. Yuan, Y. Liu, Y. Wang, Y. Wang, and H. Zhao, “Streammapnet: Streaming mapping network for vectorized online hd map construction,” in *Proceedings of the IEEE/CVF Winter Conference on Applications of Computer Vision (WACV)*, Jan. 2024, pp. 7356–7365.
- [24] K. Z. Luo, X. Weng, Y. Wang, S. Wu, J. Li, K. Q. Weinberger, et al., “Augmenting lane perception and topology understanding with standard definition navigation maps,” in *2024 IEEE International Conference on Robotics and Automation (ICRA)*, 2024, pp. 4029–4035.
- [25] X. Zhang, G. Liu, Z. Liu, N. Xu, Y. Liu, and J. Zhao, “Enhancing vectorized map perception with historical rasterized maps,” in *European Conference on Computer Vision*, 2024.
- [26] Y. Du, S. Yang, L. Wang, Z. Hou, C. Cai, Z. Tan, et al., *Rtmap: Real-time recursive mapping with change detection and localization*, 2025. arXiv: 2507.00980 [cs.CV].
- [27] A. v. d. Oord, Y. Li, and O. Vinyals, *Representation Learning with Contrastive Predictive Coding*, arXiv:1807.03748 [cs], Jan. 2019.
- [28] K. He, X. Zhang, S. Ren, and J. Sun, “Deep residual learning for image recognition,” in *2016 IEEE Conference on Computer Vision and Pattern Recognition (CVPR)*, 2016, pp. 770–778.
- [29] B. Wilson, W. Qi, T. Agarwal, J. Lambert, J. Singh, S. Khandelwal, et al., “Argoverse 2: Next generation datasets for self-driving perception and forecasting,” in *Proceedings of the Neural Information Processing Systems Track on Datasets and Benchmarks (NeurIPS Datasets and Benchmarks 2021)*, 2021.
- [30] O. Siméoni, H. V. Vo, M. Seitzer, F. Baldassarre, M. Oquab, C. Jose, et al., *DINOv3*, 2025. arXiv: 2508.10104 [cs.CV].
- [31] A. Blumberg, J. Merkert, R. Fehler, F. Immel, F. Bieder, J.-H. Pauls, et al., “Impact of localization errors on label quality for online hd map construction,” in *2025 IEEE Intelligent Vehicles Symposium (IV)*, 2025, pp. 1833–1840.
- [32] NVIDIA Corporation, *Physicalai-autonomous-vehicles dataset*, <https://huggingface.co/datasets/nvidia/PhysicalAI-Autonomous-Vehicles>, Access requires acceptance of the NVIDIA Autonomous Vehicle Dataset License Agreement, 2025.